Phase behavior of hard-core lattice gases: A fundamental measure approach

Luis Lafuente[a] and José A. Cuesta[b]
Grupo Interdisciplinar de Sistemas Complejos (GISC), Departamento de Matemáticas, Universidad Carlos III de Madrid, Avda. de la Universidad 30, 28911-Leganés, Madrid, Spain

(Received 10 June 2003; accepted 11 August 2003)

We use an extension of fundamental measure theory to lattice hard-core fluids to study the phase diagram of two different systems. First, two-dimensional parallel hard squares with edge-length $\sigma=2$ in a simple square lattice. This system is equivalent to the lattice gas with first and second neighbor exclusion in the same lattice, and has the peculiarity that its close packing is degenerated (the system orders in sliding columns). A comparison with other theories is discussed. Second, a three-dimensional binary mixture of parallel hard cubes with $\sigma_L=6$ and $\sigma_S=2$. Previous simulations of this model only focused on fluid phases. Thanks to the simplicity introduced by the discrete nature of the lattice we have been able to map out the complete phase diagram (both uniform and nonuniform phases) through a free minimization of the free energy functional, so the structure of the ordered phases is obtained as a result. A zoo of entropy-driven phase transitions is found: one-, two- and three-dimensional positional ordering, as well as fluid-ordered phase and solid-solid demixings. © *2003 American Institute of Physics.* [DOI: 10.1063/1.1615511]

I. INTRODUCTION

Hard-core systems are the paradigm of entropy-driven phase transitions. The first example of an entropy-driven (orientational) ordering transition is given in the famous Onsager's paper[1] on the isotropic-nematic transition in a three-dimensional system of thin hard rods. But probably, the best known and discussed example of entropy-driven (three-dimensional positional) ordering transition is the freezing of hard spheres. This was first devised by Kirkwood *et al.*[2] using an approximate theory, but the definite evidence about the existence of such a purely entropic transition was the numerical simulations of Alder and Wainwright,[3] and Wood and Jacobson.[4] As very few models can be solved exactly, definite conclusions on the existence of phase transitions often come from numerical simulations. But in many cases these are very demanding and powerful computers are needed in order to reach a reliable system size. This fact, together with the inexistence of appropriate theoretical approaches, could explain that until the end of the eighties there were no more instances of entropy-driven ordering transitions. At that time, a series of numerical simulations[5–7] showed that hard-core interaction can also induce one- and two-dimensional positional ordering (smectic and columnar phases, respectively, in liquid crystal terminology). This was a very striking fact, because it was generally believed that the mechanism underlying these phase transitions was the decrease of internal energy rather than the gain of entropy.

Apart from ordering transitions, it is well known that binary nonadditive mixtures can demix by a pure entropic effect. An extreme case of nonadditivity was studied by Widom and Rowlinson[8] in a model with two different species interacting ideally between members of the same species ($\sigma_{AA}=\sigma_{BB}=0$) and with a hard-core interaction between unlike particles ($\sigma_{AB}=\sigma$). They rigorously showed that the system demixes into two fluid phases with different compositions. This can be easily understood if we notice that the available volume is more effectively filled by pure phases than by the mixture. Another interesting example of this kind is found in colloid-polymer mixtures. Experimentally, it is well known that the addition of nonadsorbing polymers to a colloidal suspension induces an effective attraction between the colloidal particles that can induce the flocculation of the colloid. A simple explanation for this effect is that the clustering of colloids (large particles) leaves more free volume to the polymers (small particles), what translates into a gain of entropy. This mechanism is known as *depletion*. Many models[9–11] have been successfully introduced in order to illustrate how this effect can induce a fluid-fluid phase separation in mixtures.

Special mention merits the case of the additive binary mixture of hard spheres. The absence of a spinodal instability in the Percus-Yevick solution for this system[12] led us to believe that entropic demixing was not possible for additive mixtures. But almost 30 years later, Biben and Hansen[13] predicted such a spinodal by using a more accurate integral equation theory. Since this result, many theoretical,[14–19] simulation[20–24] and experimental[25–28] results appeared supporting the existence of demixing in additive binary mixtures of hard spheres when the diameter ratio is at least 5:1. Almost at the same time, it was pointed out that instead of a fluid-fluid demixing at least one of the separated phases might be ordered.[16–19,21–24,26–28] The actual scenario for this system is a metastable fluid-fluid demixing[23] preempted by a fluid-solid coexistence or (if the mixture is sufficiently asymmetric) a solid-solid one. Qualitatively, this is the same situ-

[a]Electronic mail: llafuent@math.uc3m.es
[b]Electronic mail: cuesta@math.uc3m.es

ation one finds in a binary additive mixture of parallel hard cubes.[29–31]

From a theoretical point of view one of the first exactly solvable hard-core models showing a fluid-solid transition was a lattice model proposed by Temperley.[32] Many other lattice hard-core models were studied in the sixties by adapting the approximate theories developed for Ising-like models to hard body systems.[33,34] They succeeded in the prediction of an order-disorder transition and mainly focused on studying the dependence of the nature of the transition upon the range of the hard-core and the topology of the underlying lattice.

For the continuum model of hard spheres, one of the most successful theories to study the freezing has been density functional theory (DFT). Many accurate functionals have been devised for the monocomponent fluid,[35] but when they are applied to the binary mixture some problems arise: (i) many of the theories employed are not directly formulated for mixtures and the extension is far from being straightforward; (ii) it is very difficult to study the solid phases because it is not trivial to determine which is the most stable structure for the mixture, and this information is an input in most approaches.[36] These difficulties have been circumvented by mapping the binary hard-core mixture into a monocomponent fluid (large particles alone) with a hard-core and an effective short-range attractive potential. It is then possible to use perturbation theory in order to study the phase diagram.[19] On the other hand, the solid phase is usually assumed to be an fcc crystal of the large particles with the small particles uniformly distributed. Although this approach has been extensively used,[21,24,37–39] it is only valid for low molar fractions of the small particles. Besides, even in this case, the assumption that the density of small particles is uniform in the ordered phase is rather unrealistic because the ordering of large particles induces structure in the distribution of the small ones. To the best of our knowledge, this problem has not been addressed satisfactorily yet.

A direct study (without resorting to an effective one-component fluid) has been carried out for a binary mixture of parallel hard cubes with Rosenfeld's fundamental measure theory[29–31] (FMT). This theory has the advantage of being naturally formulated for mixtures. A complete analysis of fluid-fluid demixing has been performed for arbitrary size ratios, but again, the lack of intuition about the distribution of small particles in the crystal makes impossible to study freezing in this system. To solve this problem one should perform a free minimization of the free energy functional and obtain the structure of the ordered phases as an output. But due to the continuum nature of the system this would require a huge amount of numerical work.

The situation is more favorable for the lattice counterpart of this model. Indeed, simulations of a binary mixture of parallel hard cubes (6:2) on a simple cubic lattice were performed by Dijkstra, Frenkel, and Hansen,[40,41] but their focus was whether entropic demixing could be observed in additive binary mixtures and the structure of the inhomogeneous phases was not considered. The results of these simulations (a stable fluid-fluid demixing) are in contradiction with the predictions of the continuum system (it exhibits a fluid-fluid spinodal only for size ratios above 10:1, and it is always preempted by freezing of the large component). With the aim of explaining this mismatch, we extended the fundamental measure functional for parallel hard cubes to the lattice version.[42] With this theory we have shown in a previous work[43] that the latter is the correct picture. (A more detailed account of this work will be given here.) Furthermore, due to the discrete nature of the system it is possible to give a complete description of the ordered phases (see below). Thus, we show that lattice models, treated in a suitable manner, can serve as a starting point to study the structure of ordered phases in (continuum) mixtures.

There is a second benefit of this extension of FMT to lattices that we want to emphasize. These simulations, together with an exactly solvable model proposed by Widom[10] and Frenkel and Louis[11] in different contexts, show that lattice models can give accurate descriptions of demixing phenomena. But in spite of their historical role in the development of Statistical Mechanics and their simplicity, with a few exceptions,[44–46] density functional theories have only focused on continuum models. We believe that the formulation of classical density functional approaches for lattice models will help to better understand both, the phase behavior of complex fluids and the formal structure of the approximate functionals.

The paper is organized as follows. A review of the lattice version of FMT is presented in Sec. II. In Sec. III, we use this theory to obtain the complete phase diagram of two systems. First, a two-dimensional system of parallel hard squares with edge-length $\sigma=2$ on a square lattice (this is equivalent to the two-dimensional lattice gas with first and second neighbor exclusion). This system has been widely studied in the literature (see Refs. 34 and 33 and references therein) and there exists a big controversy about its phase behavior so far unsettled. A detailed analysis is performed by applying the new theory, and a comparison with results from other theories is discussed. The lattice fundamental measure theory (LFMT) appears to be at the same level of accuracy of the other well accepted theories. Second, we have addressed the problem of the binary additive mixture studied by simulations, i.e., a binary mixture of parallel hard cubes ($\sigma_L=2$, $\sigma_S=6$) on a simple cubic lattice. Due to the simplification introduced by the lattice, the complete phase diagram has been mapped out. It shows a very rich collection of entropic phase transitions. As a matter of fact, we have found one-, two- and three-dimensional ordering transitions, as well as fluid-ordered phase and solid-solid demixings. A free minimization of the free energy functional has been performed, so the structure of the ordered phases has also been obtained. Finally, conclusions are discussed in Sec. IV. Notice that Refs. 42 and 43 contain a preliminary account of the work presented here in full detail.

II. THEORY

The construction of the lattice fundamental measure functional is based on the ideas of the exact zero-dimensional reduction[47,48] and in the exact form of the one-dimensional functional. A full account of the details of the procedure can be found in Ref. 42. In that work, the general

form of the functional for a system of parallel hard cubes in a simple cubic lattice (for any dimension, particle size or number of components) is presented. Basically, the idea behind it is to construct a family of functionals for arbitrary dimension in such a way that they consistently satisfy the dimensional reduction property of the exact functionals down to zero-dimensional cavities (i.e., cavities which can host no more than one particle). Moreover, the prescription chosen is inspired in the exact functional for the one-dimensional system, which is recovered with the scheme proposed.

Let us consider a d-dimensional additive mixture of parallel hypercubes with edge-lengths $\sigma_\alpha = 2a_\alpha + \epsilon$ lattice spacings, where α is the species index and $\epsilon = 0,1$ does not depend on α, i.e., all the species have, simultaneously, even or odd sizes (the mixed—nonadditive—case is more involved,[42] so we just ignored it because it will not be used anywhere in this work). In Ref. 42 the excess free energy functional for this system in this approximation was found to be [cf. Eq. (3.2) of that reference]

$$\beta\mathcal{F}_{\mathrm{ex}}[\rho] = \sum_{\mathbf{s}\in\mathbb{Z}^d} \sum_{\mathbf{k}\in\{0,1\}^d} (-1)^{d-k} \Phi_0(n^{(\mathbf{k})}(\mathbf{s})), \tag{1}$$

where $k = \Sigma_{l=1}^d k_l$, $\Phi_0(\eta) = \eta + (1-\eta)\ln(1-\eta)$ is the excess free energy for a zero-dimensional cavity with mean occupancy $0 \leqslant \eta \leqslant 1$, β the reciprocal temperature in Boltzmann's units and $n^{(\mathbf{k})}(\mathbf{s})$ are weighted densities defined by the convolutions

$$n^{(\mathbf{k})}(\mathbf{s}) = \sum_\alpha \sum_{\mathbf{r}\in\mathbb{Z}^d} w_\alpha^{(\mathbf{k})}(\mathbf{s}-\mathbf{r})\rho_\alpha(\mathbf{r}), \tag{2}$$

$\rho_\alpha(\mathbf{s})$ being the one-particle distribution function for species α and

$$w_\alpha^{(\mathbf{k})}(\mathbf{s}) = \prod_{l=1}^d w_\alpha^{(k_l)}(s_l), \tag{3}$$

$$w_\alpha^{(k)}(s) = \begin{cases} 1 & \text{if } -a_\alpha - k - \epsilon < s < a_\alpha, \\ 0 & \text{otherwise.} \end{cases} \tag{4}$$

Notice that as weights are indexed by $\mathbf{k}\in\{0,1\}^d$, there are 2^d different weighted densities.

The direct correlation function between species α and γ can be obtained from this functional as

$$c_{\alpha\gamma}(\mathbf{s}-\mathbf{r}) = -\left.\frac{\partial^2 \beta\mathcal{F}_{\mathrm{ex}}[\rho]}{\partial\rho_\alpha(\mathbf{s})\partial\rho_\gamma(\mathbf{r})}\right|_{\mathrm{uniform}}.$$

Then, from Eq. (1),

$$c_{\alpha\gamma}(\mathbf{s}) = -\sum_{\mathbf{k}\in\{0,1\}^d} \frac{(-1)^{d-k}}{1-n_k} \varphi_{\alpha\gamma}^{(\mathbf{k})}(\mathbf{s}), \tag{5}$$

where $n_k = \Sigma_\alpha \sigma_\alpha^k (\sigma_\alpha - 1)^{d-k}\rho_\alpha$ are the weighted densities (2) in the uniform limit and $\varphi_{\alpha\gamma}^{(\mathbf{k})}(\mathbf{s})$ is the convolution

$$\varphi_{\alpha\gamma}^{(\mathbf{k})}(\mathbf{s}) \equiv \sum_{\mathbf{r}\in\mathbb{Z}^d} w_\alpha^{(\mathbf{k})}(\mathbf{r}) w_\gamma^{(\mathbf{k})}(\mathbf{r}+\mathbf{s}). \tag{6}$$

Because of the structure of the direct correlation function it is convenient to work with its discrete Fourier transform, which takes the form

$$\hat{c}_{\alpha\gamma}(\mathbf{q}) = -\sum_{\mathbf{k}\in\{0,1\}^d} \frac{(-1)^{d-k}}{1-n_k} \hat{w}_\alpha^{(\mathbf{k})}(-\mathbf{q}) \hat{w}_\gamma^{(\mathbf{k})}(\mathbf{q}), \tag{7}$$

where

$$\hat{w}_\alpha^{(\mathbf{k})}(\mathbf{q}) = \prod_{l=1}^d e^{-i\,q_l/2\,k_l} \frac{\sin q_l\left(a_\alpha + \dfrac{k_l - 1}{2}\right)}{\sin q_l/2}. \tag{8}$$

The general expression of the functional (1) adopts very simple forms when particularized to specific systems. In order to make clear the structure of the functional, we will introduce a diagrammatic notation which helps visualizing its dimensional reduction properties in a simple way. For the sake of simplicity let us consider the lattice gas with first and second neighbor exclusion in a two-dimensional square lattice. This is a system of parallel hard squares with $\sigma = 2$ lattice spacings. In diagrammatic notation the excess free energy functional (1) can be written

$$\beta\mathcal{F}_{\mathrm{ex}}[\rho] = \sum_{\mathbf{s}\in\mathbb{Z}^2} [\Phi_0(\square) - \Phi_0(\circ\!\!-\!\!\circ) - \Phi_0(\overset{\circ}{\circ}) + \Phi_0(\circ)], \tag{9}$$

where the diagrams represent the weighted densities (2) as

$$\square = n^{(1,1)}(\mathbf{s}) = \rho(s_1,s_2) + \rho(s_1+1,s_2) + \rho(s_1,s_2+1) + \rho(s_1+1,s_2+1),$$

$$\circ\!\!-\!\!\circ = n^{(1,0)}(\mathbf{s}) = \rho(s_1,s_2) + \rho(s_1+1,s_2),$$

$$\overset{\circ}{\circ} = n^{(0,1)}(\mathbf{s}) = \rho(s_1,s_2) + \rho(s_1,s_2+1),$$

$$\circ = n^{(0,0)}(\mathbf{s}) = \rho(s_1,s_2). \tag{10}$$

What becomes apparent with this diagrammatic notation is that the excess functional (1) can be regarded as a linear combination of contributions due to a particular set of zero-dimensional cavities (10). Furthermore, we can manipulate the diagrams in order to prove the dimensional reduction properties that the functional (9) satisfies. To illustrate this, we will consider the dimensional reduction to a one-dimensional system, the hard rod lattice gas, whose exact excess functional is known to have the form (1).[42] To perform this reduction, we will apply an infinite external potential in every site of the lattice except in an infinite linear chain defined by $\mathcal{L} = \{(s_1,0): s_1 \in \mathbb{Z}\}$. This implies that the centers of mass of the particles can only occupy the sites in $\mathcal{L}$, the system becoming equivalent to a hard rod lattice gas with particles of size $\sigma = 2$. In terms of $\rho(\mathbf{s})$ this means that $\rho(\mathbf{s}) = \rho(s_1)\delta_{s_2,0}$, where $\delta_{i,j}$ is the Kronecker symbol and $\rho(s)$ is the one-particle distribution function for the one-dimensional system. Within this constraint, the excess free-

energy functional of the effective system can be obtained by summing over $s_2 \in \mathbb{Z}$ in Eq. (9). Each contribution gives, respectively,

$$\sum_{s_2 \in \mathbb{Z}} \Phi_0(\boxplus) = 2\Phi_0(\circ\!\!-\!\!\circ),$$

$$\sum_{s_2 \in \mathbb{Z}} \Phi_0(\circ\!\!-\!\!\circ) = \Phi_0(\circ\!\!-\!\!\circ),$$

$$\sum_{s_2 \in \mathbb{Z}} \Phi_0(\overset{\circ}{\circ}) = 2\Phi_0(\circ),$$

$$\sum_{s_2 \in \mathbb{Z}} \Phi_0(\circ) = \Phi_0(\circ),$$

where the diagrams in the r.h.s. must now be interpreted as $\circ\!\!-\!\!\circ = \rho(s) + \rho(s+1)$ and $\circ = \rho(s)$. Therefore, the excess free-energy functional for the one-dimensional system so obtained is

$$\beta \mathcal{F}_{\text{ex}}^{(1d)}[\rho] = \sum_{s_1 \in \mathbb{Z}} [\Phi_0(\circ\!\!-\!\!\circ) - \Phi_0(\circ)], \tag{11}$$

which coincides with the exact result [see Eqs. (2.26) and (3.1) of Ref. 42].

Another example in three-dimensions is given in the Appendix.

III. APPLICATIONS

In spite of the simple structure of the lattice fundamental measure functionals, the applications to specific systems have proven able to describe very complex phase diagrams.[43] In this section we will study in detail two particular systems: first, the lattice gas with exclusion to first and second neighbors on a square lattice; second, a binary mixture of parallel hard cubes with $\sigma = 2$ and 6, in a simple cubic lattice.

A. Parallel hard squares

This model is defined by the interaction pair potential

$$\phi(\mathbf{s}, \mathbf{s}') = \begin{cases} \infty & \text{if } |s_i - s_i'| \leqslant 1 \text{ for both } i = 1,2, \\ 0 & \text{otherwise.} \end{cases} \tag{12}$$

It has been previously studied employing other approximate theories, such as finite-size scaling methods,[49,50] series expansions[51–53] and clusters methods.[33,51] All authors agree in that the close-packed state is a columnar phase (ordered along one dimension but fluid along the other). This notwithstanding, the nature of the transition remains doubtful, the results being highly dependent on the theory used.[34] While some authors conclude that the system exhibits a third order transition very near close packing,[49,51–53] others obtain a second order transition at a lower density,[33,51,54] and even some of them have speculated about the lack of such a phase change.[50,51,54] The results obtained with the present theory are in accordance with those of the second order phase transition. Unfortunately, we have no concluding arguments to umpire this dispute.

The advantage of our approach over other theories is that it provides a simple prescription to build a density functional in closed form. Then, all the powerful tools of density functional theory may be applied. The excess functional for this system within the present theory is that of Eq. (9).

In order to pin down the phase diagram of the system we will proceed systematically: first, studying the uniform phases, and second, considering spatial inhomogeneities. For a uniform density profile $\rho(\mathbf{s}) = \rho$, the weighted densities (10) become $\boxplus = 4\rho$, $\circ\!\!-\!\!\circ = \overset{\circ}{\circ} = 2\rho$ **and** $\circ = \rho$, where $0 \leqslant \rho \leqslant 1/4$. The excess free energy density (in $k_B T$ units) can be calculated particularizing Eq. (9), which yields

$$\Phi_{\text{ex}}(\rho) = \Phi_0(4\rho) - 2\Phi_0(2\rho) + \Phi_0(\rho). \tag{13}$$

Adding up the ideal gas contribution, $\Phi_{\text{id}} = \rho(\ln \rho - 1)$, and taking into account the definition of Φ_0, we obtain the following free energy density for the fluid

$$\Phi_{\text{fluid}}(\rho) = \rho \ln \rho + (1-\rho)\ln(1-\rho) + (1-4\rho)\ln(1-4\rho) - 2(1-2\rho)\ln(1-2\rho). \tag{14}$$

From this, all the thermodynamic properties of the fluid phase can be derived. For instance, the fugacity is given by

$$z_{\text{fluid}} = \frac{\rho(1-2\rho)^4}{(1-\rho)(1-4\rho)^4}, \tag{15}$$

and the pressure takes the simple form

$$\beta p_{\text{fluid}} = \ln\left[\frac{(1-2\rho)^2}{(1-\rho)(1-4\rho)}\right]. \tag{16}$$

The structure of the equilibrium phase can be analyzed by means of the direct correlation function, obtained from Eq. (5) particularizing for $d = 2$ and a single component with $\sigma = 2$. In a symmetry broken continuous phase transition, for some $\mathbf{q} \neq \mathbf{0}$

$$1 - \rho \hat{c}(\mathbf{q}) = 0, \tag{17}$$

this condition being equivalent to the divergence of the structure factor. Since we are interested in the spatial instabilities of the uniform phase, we have to look for the lowest value of ρ which makes the condition (17) solvable for some $\mathbf{q}$. Taking into account that the symmetry of the system enables us to take $\mathbf{q} = (q, 0)$, Eq. (17) becomes

$$\cos^2(q/2) = -\frac{1 - \dfrac{4\rho}{1-2\rho} + \dfrac{\rho}{1-\rho}}{4\rho\left(\dfrac{4}{1-4\rho} - \dfrac{1}{1-2\rho}\right)}. \tag{18}$$

Since the denominator is positive in the whole range of ρ, and so is the numerator for small values of the density, the solution corresponds to the vanishing of the latter. This occurs at the density

$$\rho_{\text{crit}} = \frac{3 - \sqrt{5}}{4} \approx 0.1910, \tag{19}$$

and, of course, $q = \pi$, implying the periodicity of the inhomogeneous phase to be $d = 2\pi/q = 2$ lattice spacings.

What remains to be determined is the symmetry of the nonuniform phase at the transition point. Based on the pre-

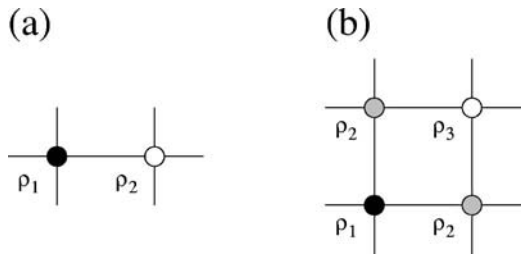

FIG. 1. The unit cell for a columnar phase with periodicity equal to two lattice spacings is shown in (a), and for a solid phase with the same periodicity in (b).

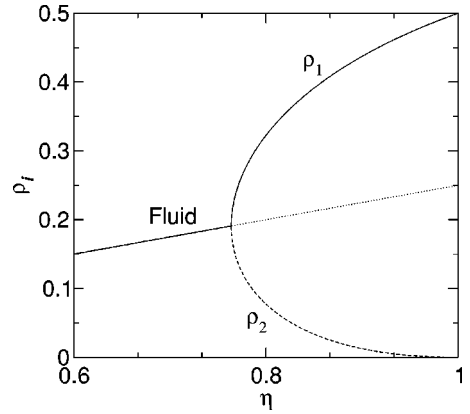

FIG. 2. Sublattice densities for the columnar phase. It also shows the metastable fluid beyond the transition point.

vious results for this system and on those recently obtained for parallel hard cubes in the continuum,[55] we guess that this phase must be either a columnar or a solid (ordering along the two coordinate axes). In order to determine which phase is the stable one, we have performed a global minimization of the functional (9) within the constraints imposed by the symmetry and periodicity of both the columnar and the solid phases. For a generic columnar phase with periodicity equal to two lattice spacings, the one-particle distribution function takes the form

$$\rho_{\mathrm{col}}(\mathbf{s})=\begin{cases}\rho_1 & \text{if } s_1 \text{ is even,}\\ \rho_2 & \text{otherwise,}\end{cases} \tag{20}$$

while for a solid phase with the same periodicity we have

$$\rho_{\mathrm{sol}}(\mathbf{s})=\begin{cases}\rho_1 & \text{if } s_1 \text{ and } s_2 \text{ are even,}\\ \rho_2 & \text{if } s_1 \text{ or } s_2 \text{ is odd,}\\ \rho_3 & \text{otherwise.}\end{cases} \tag{21}$$

A sketch of the unit cell for each case is shown in Fig. 1. Note that the uniform phase is included in both Eqs. (20) and (21).

For the columnar phase the total free energy density takes the form

$$\begin{aligned}\Phi_{\mathrm{col}}(\rho_1;\rho)=&\Phi_{\mathrm{id}}(\rho_1,2\rho-\rho_1)+\Phi_0(4\rho)-\Phi_0(2\rho)\\&-\tfrac{1}{2}[\Phi_0(2\rho_1)+\Phi_0(4\rho-2\rho_1)-\Phi_0(\rho_1)\\&-\Phi_0(2\rho-\rho_1)],\end{aligned} \tag{22}$$

where we have substituted the density profile (20) in Eq. (9), used the relation $2\rho=\rho_1+\rho_2$, and introduced the ideal term $\Phi_{\mathrm{id}}(\rho_1,\rho_2)=\frac{1}{2}\Sigma_i\rho_i(\ln\rho_i-1)$.

We can now minimize the total free energy density at constant ρ. Note that in this case we have to minimize with respect to a single variable. The Euler-Lagrange equation is

$$\frac{\rho_1(1-2\rho_1)^2(1-2\rho+\rho_1)}{(2\rho-\rho_1)(1-4\rho+2\rho_1)^2(1-\rho_1)}=1. \tag{23}$$

One solution corresponds to the uniform phase ($\rho_1^{\mathrm{eq}}=\rho$). It can be easily checked that this is indeed the minimum of the free energy for $\rho<\rho_{\mathrm{crit}}$, as expected. After removing this solution from Eq. (23), we obtain a quadratic polynomial whose roots become physical for $\rho\geqslant\rho_{\mathrm{crit}}$. Above the critical density the uniform phase is no longer a minimum; instead, we have a columnar phase given by (see Fig. 2)

$$\rho_1^{\mathrm{eq}}=\rho+\frac{1}{2}\sqrt{\frac{(1-2\rho)(\rho-\rho_{\mathrm{crit}})(3-2\rho-2\rho_{\mathrm{crit}})}{\rho}} \tag{24}$$

(we have chosen $\rho_1^{\mathrm{eq}}>\rho_2^{\mathrm{eq}}=2\rho-\rho_1^{\mathrm{eq}}$). This phase has a lower free energy than the fluid phase for $\rho>\rho_{\mathrm{crit}}$, but we still have to calculate free energy for the solid branch in order to know which one is the stable phase above the transition point.

For the solid phase, substituting Eq. (21) in Eq. (9) and adding the ideal contribution, the total free energy density turns out to be

$$\begin{aligned}\Phi_{\mathrm{sol}}(\rho_1,\rho_3;\rho)=&\Phi_{\mathrm{id}}(\rho_1,2\rho-\rho_+,\rho_3)+\Phi_0(4\rho)\\&-\Phi_0(2\rho+\rho_-)-\Phi_0(2\rho-\rho_-)\\&+\tfrac{1}{4}[\Phi_0(\rho_1)+2\Phi_0(2\rho-\rho_+)+\Phi_0(\rho_3)],\end{aligned} \tag{25}$$

where we have used $4\rho=\rho_1+2\rho_2+\rho_3$ to eliminate the dependence on ρ_2, and have defined $\rho_\pm=(\rho_1\pm\rho_3)/2$. As in the previous case, the equilibrium density profile is the global minimum of Eq. (25) at constant ρ, but now we have two independent variables, ρ_1 and ρ_3. Thus, the Euler-Lagrange equations are now the system of algebraic equations

$$\begin{aligned}&\frac{\rho_1(1-2\rho-\rho_-)^2(1-2\rho+\rho_+)}{(1-\rho_1)(2\rho-\rho_+)(1-2\rho+\rho_-)^2}=1,\\&\frac{\rho_3(1-2\rho+\rho_-)^2(1-2\rho+\rho_+)}{(1-\rho_3)(2\rho-\rho_+)(1-2\rho-\rho_-)^2}=1.\end{aligned} \tag{26}$$

The fluid phase, given by $\rho_1^{\mathrm{eq}}=\rho_3^{\mathrm{eq}}=\rho$, is the solution for $\rho\leqslant\rho_{\mathrm{crit}}$. The solution for $\rho\geqslant\rho_{\mathrm{crit}}$ must be obtained numerically and is plotted in Fig. 3. In Fig. 4 we can see that the solid branch bifurcates with a free energy lower than that of the fluid phase, but larger than that of the columnar phase. The transition is then fluid-columnar.

It is feasible to study analytically the behavior of each branch at the transition point. This would give a definite conclusion about the nature of the phase change. It is straightforward to check the continuity of $d\Phi/d\rho$ at ρ_{crit} (for both the solid and the columnar branches), but a discontinuity is found in the second derivative at ρ_{crit}, so the transition

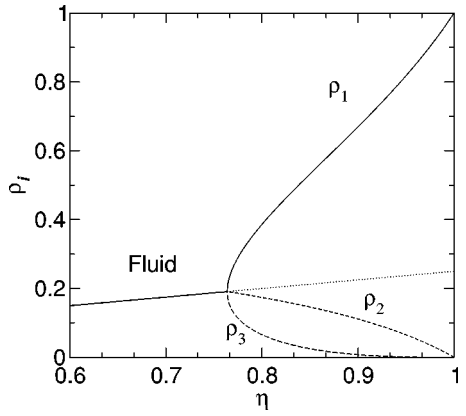

FIG. 3. Sublattice densities for the solid phase. It is also shown the metastable fluid beyond the transition point.

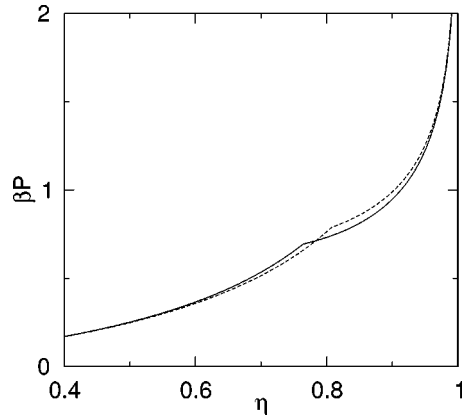

FIG. 5. Equation of state of the hard square fluid from lattice fundamental measure theory (solid line) and from the cluster method of Rushbrooke and Scoins (dashed line).

is second order. Furthermore, the stable phase beyond the transition point is the one with lowest second derivative for $\rho \to \rho_{\text{crit}}^{+}$. From the values

$$\begin{aligned} \Phi''_{\text{fluid}}(\rho_{\text{crit}}^{+}) &= 2(15+7\sqrt{5}) \approx 61.3, \\ \Phi''_{\text{col}}(\rho_{\text{crit}}^{+}) &= 2(5+2\sqrt{5}) \approx 18.9, \\ \Phi''_{\text{sol}}(\rho_{\text{crit}}^{+}) &= 4(5+\sqrt{5}) \approx 28.9, \end{aligned} \tag{27}$$

we conclude that indeed the system undergoes a second order transition from a fluid phase to a columnar one at ρ_{crit}. Besides, as it can be inferred from the density dependence of the free energy density for every branch (Fig. 4), the columnar phase remains the most stable phase up to close packing.

We can now plot the equation of state (Fig. 5), with the fluid branch given by Eq. (16) and the columnar one by

$$\beta p_{\text{col}} = \frac{1}{2} \ln \left[\frac{(1-2\rho)^2 (1-2\rho_1^{\text{eq}})(1-4\rho+2\rho_1^{\text{eq}})}{(1-4\rho)^2 (1-\rho_1^{\text{eq}})(1-2\rho+\rho_1^{\text{eq}})} \right]. \tag{28}$$

The fugacity of the columnar phase is given by

$$z_{\text{col}} = \frac{\rho_1^{\text{eq}} (1-2\rho)^2 (1-2\rho_1^{\text{eq}})^2}{(1-4\rho)^4 (1-\rho_1^{\text{eq}})}. \tag{29}$$

At the critical point, we have

$$\beta p_{\text{crit}} = \ln 2, \quad z_{\text{crit}} = \frac{11+5\sqrt{5}}{2}. \tag{30}$$

As mentioned at the beginning of this section, the results from this lattice fundamental measure theory are compatible with the ones obtained by Bellemans and Nigam[51] ($\rho_{\text{crit}} \approx 0.202$, $\beta p_{\text{crit}} \approx 0.788$ and $z_{\text{crit}} \approx 17.29$) through the cluster method of Rushbrooke and Scoins[56] (plotted with a dashed line in Fig. 5). From Fig. 5 we can see that the agreement at low and high densities is very accurate, and deviations occur only near the critical point. This can be understood if we realize that both theories neglect correlations beyond a certain distance between the particles, so a very accurate description of the critical properties should not be expected. This notwithstanding, as remarked by Runnels,[34] due to the degeneracy of the close-packed configuration, this system is difficult to study with finite-size or series expansions methods, and a closed-form approximation could be superior at describing the correct phase behavior.

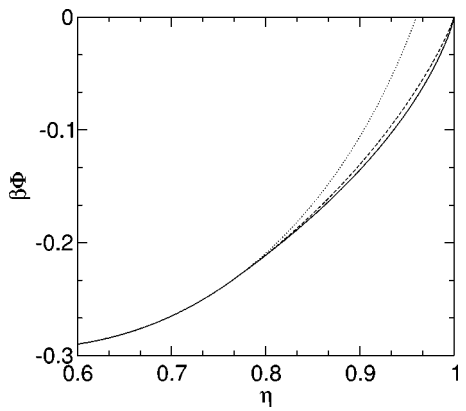

FIG. 4. Free energy density of the fluid (dotted line), columnar (solid line) and solid (dashed line) phases.

B. Multicomponent system of parallel hard cubes

Let us now consider a multicomponent hard cube lattice gas in a simple cubic lattice. If we denote $\sigma_1, \ldots, \sigma_p$ the edge-lengths of the different species, then the interaction potential between species α and γ, will be given by

$$\phi_{\alpha\gamma}(\mathbf{s},\mathbf{s}') = \begin{cases} \infty & \text{if } \max_{i=1,2,3} |s_i - s_i'| \leqslant \frac{1}{2}(\sigma_\alpha + \sigma_\gamma), \\ 0 & \text{otherwise.} \end{cases} \tag{31}$$

The lattice fundamental measure approximation for the free energy functional of this system has already been reported in Ref. 42 [Eqs. (3.2) and (3.3) of that reference], together with the phase diagram for the particular case of a binary mixture with $\sigma_L = 6$ and $\sigma_S = 2$, but no details about the calculation were given. In this subsection we will study the phase behavior of the general uniform mixture and obtain the complete bulk phase diagram, including both uniform and ordered phases, for the particular case just mentioned.

In the uniform regime, the one-particle distribution function no longer depends on the spatial variables: $\rho_\alpha(\mathbf{s})=\rho_\alpha$, $\alpha=1,\ldots,p$. In this case, the free energy density has the simple form[42]

$$\Phi(\rho_1,\ldots,\rho_p)=\sum_{\alpha=1}^{p}\rho_\alpha(\ln\rho_\alpha-1)+\Phi_0(n_3)-\Phi_0(n_2)+\Phi_0(n_1)-\Phi_0(n_0) \tag{32}$$

[with the densities n_k defined below Eq. (5)].

As it is well known, the stability of the mixture is determined by the matrix

$$\mathsf{M}_{\alpha\gamma}=\frac{\partial^2\Phi}{\partial\rho_\alpha\partial\rho_\gamma}. \tag{33}$$

In order for the system to be stable in a mixed state this matrix must be positive definite. As this requirement is fulfilled in the low density limit, the spinodal curve can be determined through the equation $\det\mathsf{M}=0$. When the excess free energy density of the system depends on the densities only via the finite set of moments $\xi_l=\Sigma_\alpha\sigma_\alpha^l\rho_\alpha$ $(l=0,\ldots,m)$, the spinodal can be expressed in the equivalent, but more suitable form[57] $\det\mathsf{Q}=0$, where

$$\mathsf{Q}_{ij}=\delta_{ij}+\sum_{k=0}^{m}\xi_{i+k}\Phi_{kj},\quad \Phi_{ij}=\frac{\partial^2\Phi_{\mathrm{ex}}}{\partial\xi_i\partial\xi_j}. \tag{34}$$

This is just our case, because the excess free energy density [the Φ_0 contributions in Eq. (32)] depends on the densities through the set $\{n_k\}$, and this variables can easily be expressed in terms of the set of moments $\{\xi_0,\ldots,\xi_3\}$. Thus the equation for the spinodal of our system reads

$$(1+2\xi_3)^2-(\xi_1+3\xi_2)(1+2\xi_3)-3(\xi_2-\xi_1)(1+\xi_4)+\xi_2(5\xi_2-\xi_1)=0. \tag{35}$$

For a binary mixture with the small component having $\sigma_S=2$, it can be shown that the smallest size ratio, $r=\sigma_L/\sigma_S$, necessary to have a spinodal instability is $r=13$. This value is in strong disagreement with previous simulation results,[40,41] which reported a demixing phase transition for $r=3$. An explanation of this mismatch has already been provided in Ref. 43 and will become clear later on.

Some spinodals for different size ratios are shown in Fig. 6. It should be noticed that the continuum counterpart[31] is recovered in the limit $\sigma_S\to\infty$, while keeping r constant. For that system, it was shown that the minimum value of r to find demixing is $r=5+\sqrt{24}\approx 9.98$. Therefore, we can conclude that the lattice enhances the stability of the mixture. What this analogy with the continuum system suggests is that we should expect fluid-fluid demixing to be preempted by the freezing of one of the coexisting phases also in the lattice model. It must be remarked that, unlike in the continuum case, in the lattice system the stability condition involves not only the size ratio, but also the edge-length of one of the components, thus making the analysis of the stability more complex.

The discrete nature of this system provides a very suitable framework to study ordering transitions. In the continuum, only a partial analysis have been done,[31] because the minimization of the functional becomes a numerically very demanding task. Usually this minimization is performed by restricting the density profiles into a parametric class, and then minimizing with respect to one or a few parameters. The problem for the mixture is that it is very difficult to guess the appropriate class. In contrast, the situation in the lattice is easier to handle because it is feasible to perform a free minimization with the only constraints imposed by the symmetry of the ordered phase and its periodicity. As it was shown in the analysis of the two-dimensional system, the periodicity of the ordered phase can be estimated from the divergence of the structure factor, in the case of a mixture the latter being a matrix. The analog to the condition (17) for the mixture is

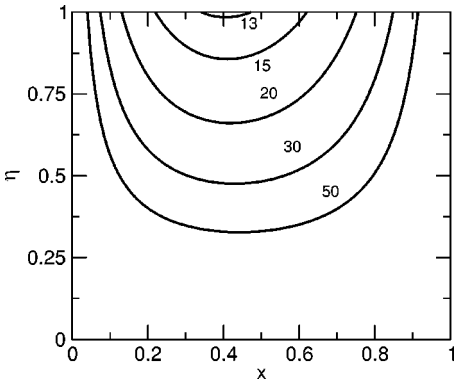

FIG. 6. Spinodal curves for a uniform binary mixture with the smallest component of size $\sigma_S=2$ and different values of the size ratio, $r=\sigma_L/\sigma_S$.

$$\det(\mathsf{P}^{-1}-\hat{\mathsf{C}}(\mathbf{q}))=0, \tag{36}$$

where $\mathsf{P}=(\delta_{\alpha\gamma}\rho_\alpha)$, a diagonal matrix, and $\hat{\mathsf{C}}(\mathbf{q})=(\hat{c}_{\alpha\gamma}(\mathbf{q}))$ is the matrix of Fourier transforms of the direct correlation functions between all species.

In the remaining of this subsection we will restrict ourselves to the particular case of the binary mixture with $\sigma_S=2$ and $\sigma_L=6$, the only case for which simulations are available.[40,41] The main result of these simulations is that the mixture undergoes an entropy-driven fluid-fluid demixing, thus being the only known example of an athermal additive model showing this feature.

The strategy we have adopted in order to obtain the complete phase diagram for the mixture has been the following: (i) First, we have calculated the phase diagram for the pure component systems, both for the small and large particles; (ii) then, we have obtained the curves marking spatial instabilities for the whole mixture through the divergence of the structure factor matrix, and have calculated the periodicity of the ordered phases arising at the bifurcation points; and (iii) finally, we have completed the phase diagram by calculating all the possible phase transitions compatible with the results obtained in the two previous steps, choosing those thermodynamically more stable.

For the pure component systems, we will proceed as in the two-dimensional case. For $\sigma=2$, the fundamental measure excess free energy functional (1) is given in diagrammatic notation in Eq. (A1). For a general one-component

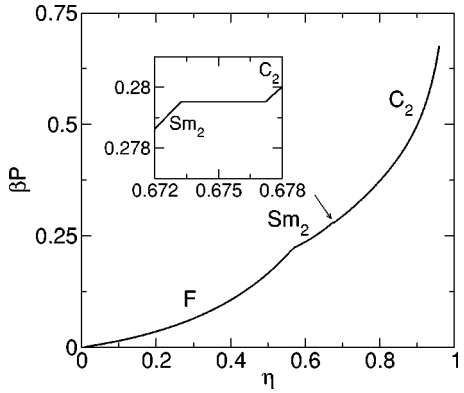

FIG. 7. Equation of state (pressure vs packing fraction) for a $\sigma=2$ parallel hard cube lattice gas on a simple cubic lattice. The different symmetries are denoted by F, Sm and C, meaning fluid, smectic and columnar, respectively. The periodicity has been indicated by a subindex. The inset shows a very narrow first order transition from a smectic to a columnar phase.

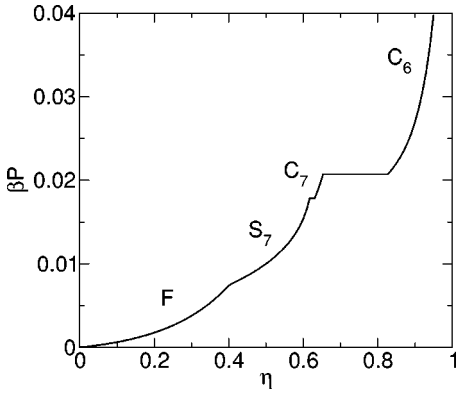

FIG. 8. Equation of state (pressure vs. packing fraction) for a $\sigma=6$ parallel hard cube lattice gas on a simple cubic lattice. The different symmetries are denoted by F, Sm, C and S, meaning fluid, smectic, columnar and solid, respectively. The periodicity has been indicated by a subindex.

system with edge-length σ, the functional form is obtained particularizing Eq. (1), but the structure is the same as that of Eq. (A1).

As it was mentioned in the previous subsection, in a symmetry broken continuous phase transition condition (17) is satisfied. For $\sigma=2$ it yields

$$\eta_{\text{crit}}=\sigma^3\rho_{\text{crit}}=0.568, \tag{37}$$

with $q=\pi$ indicating a periodicity $d=2\pi/q=2$, while for $\sigma=6$ we find the value

$$\eta_{\text{crit}}=\sigma^3\rho_{\text{crit}}=0.402, \tag{38}$$

and period $d=7$. Notice that at close packing this system has period $d=6$, so we must consider both. With respect to the symmetry of the phases, we have considered the smectic, columnar and solid ones (ordering along one, two and three coordinate axes, respectively).

Now it is possible to perform a free minimization of the functional with the above restrictions. In this case we have to proceed numerically, because the complexity of the problem does not permit an analytical treatment. This notwithstanding, the structural form of the functional simplifies the numerical work: the weighted densities are just convolutions which can be computed by using fast Fourier transform. To give an idea about the degree of complexity of the problem we will say that the simplest phase to minimize is the period-2 smectic, which involves minimization on two variables, and the most complex one is the period-7 solid, which involves minimization on twenty variables.

The phase diagrams of both systems, $\sigma=2$ and $\sigma=6$, are shown in Figs. 7 and 8, respectively. Also, the free energy density near the critical point appears in Figs. 9 and 10, respectively. From these figures, we can see that there exists a strong competition between the different phases. This reflects in the very narrow first order transitions observed in the phase diagrams, such as the Sm_2-C_2 coexistence ($\eta_{\text{Sm}_2}=0.673$ and $\eta_{C_2}=0.677$) in the $\sigma=2$ system, and the S_7-C_7 ($\eta_{S_7}=0.617$ and $\eta_{C_7}=0.631$) for $\sigma=6$. Since our treatment is approximate, these phase transitions could actually be spurious: given the small differences between the free energy densities of the phases involved, other scenarios might be possible. In contrast, there also exists very well defined transitions which offer higher confidence, such as the C_7-C_6 first order transition ($\eta_{C_7}=0.656$ and $\eta_{C_6}=0.827$) in the $\sigma=6$ system.

Let us now consider the binary mixture with $\sigma_L=6$ and $\sigma_S=2$. From the discussion about the uniform multicomponent system we can conclude that, for a size ratio $r=3$ and a small particle edge-length $\sigma_S=2$, there is no fluid-fluid demixing (not even metastable). Then, we have to look for spatial instabilities. To this purpose we must study condition (36). The direct correlation function is now a 2×2 matrix whose elements are given by Eq. (5). If we characterize the thermodynamics of our system by the total packing fraction $\eta=\eta_L+\eta_S$, where $\eta_{L(S)}=\sigma^3_{L(S)}\rho_{L(S)}$ is the packing fraction of the large (small) cubes, and by the composition $x=\eta_L/\eta$, then, for every value of x, we have to look for the smallest value of η which makes the condition (36) solvable. The solution is plotted in Fig. 11. (Fig. 12 shows the same phase diagram with η replaced by the pressure.) It should be remarked that for $0\leqslant x\leqslant 0.728$ the period of the ordered phases at the fluid spinodal is $d=2$, while for $1\geqslant x\geqslant 0.728$ we have found $d=7$.

With this guidance we can start looking for the true phase diagram. This is a very demanding numerical task, but feasible in a reasonable amount of time. For each coexistence curve involving, say, phases P_1 and P_2, we have to solve the equilibrium equations

$$\begin{aligned}
&\beta p(\eta_{P_1},x_{P_1})=\beta p(\eta_{P_2},x_{P_2}),\\
&z_L(\eta_{P_1},x_{P_1})=z_L(\eta_{P_2},x_{P_2}),\\
&z_S(\eta_{P_1},x_{P_1})=z_S(\eta_{P_2},x_{P_2}).
\end{aligned} \tag{39}$$

Every iteration of the procedure requires the minimization of the functional, at constant η and x, for both phases. In the simplest case this corresponds to a minimization problem with four variables, but in the most complicated case we have to deal with a forty variable minimization. Another problem we find is that the subtle differences between the free energy of different phases, already encountered in the monocomponent systems, make it very hard to discern which

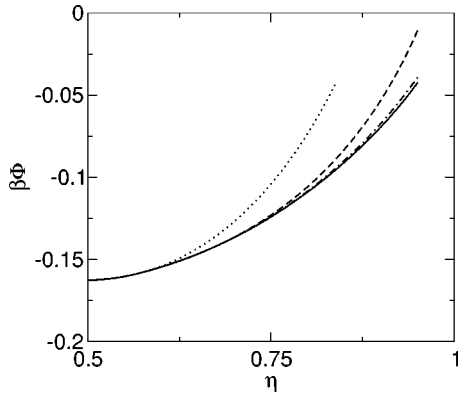

FIG. 9. Free energy density of the fluid (dotted line), smectic (dashed line), columnar (solid line) and solid (dotted-dashed line) phases, for the system of hard cubes with $\sigma=2$ in a simple cubic lattice.

one is the most stable phase. So, in many cases it is not clear which coexistence is thermodynamically more stable. In these doubtful cases, we have resorted to the Gibbs free energy per particle, $g(p,X)=X\mu_L+(1-X)\mu_S$, where $\mu_{L,S}$ is the chemical potential of each species and $X\equiv\rho_L/\rho=x/(r+(1-r)x)$ is the molar fraction. When $g(p,X)$ is plotted at constant pressure as a function of X, the coexisting phases in the mixture can be found through a double tangent construction.

The complete phase diagram appears in Figs. 11 and 12 in two different representations. In Fig. 12, it can be observed (see the insets) that there exist very small parts on the phase diagram with a plethora of very narrow coexistence regions. As in the monocomponent case, many of them could just be spurious. One of the most remarkable features is that there exists a wide phase separation between a small-particle-rich fluid phase and a large-particle-rich columnar phase (which becomes a solid phase for higher pressures). As explained in the Introduction, this is the usual scenario for this kind of mixtures. The revision of the simulations (also shown in Fig. 11) resulting from this phase behavior has already been discussed in detail in Ref. 43. The main consequence of this comparison is that some of the state points obtained in the simulations must have been misinterpreted as

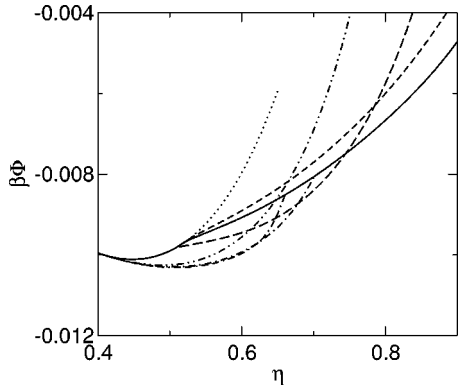

FIG. 10. Free energy density of the fluid (dotted line), smectic (double dotted-dashed line), columnar (dotted-dashed line) and solid (double dashed-dotted line) phases with periodicity $d=7$ and smectic (long-dashed line), columnar (solid line) and solid (dashed line) phases with periodicity $d=6$, for the same system of the previous figure but with $\sigma=6$.

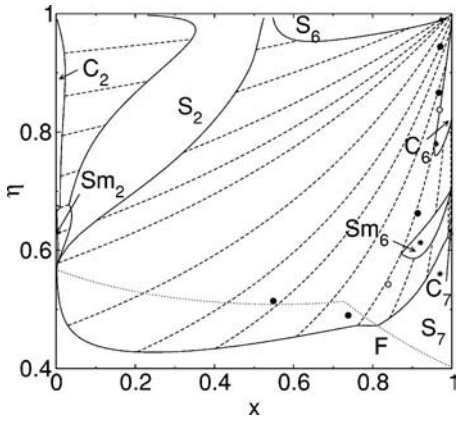

FIG. 11. Phase diagram of the binary mixture of parallel hard cubes (size ratio 6:2), $\eta=\eta_L+\eta_S$ being the total packing fraction of the large (L) and small (S) cubes, and $x=\eta_L/\eta$. The phases are labeled F (fluid), Sm_α (smectic), C_α (columnar), and S_α (solid), where $\alpha=2,6,7$ stands for the periodicity of the ordered phases. The dashed lines join coexisting states. The dotted line corresponds to the spinodal of the uniform fluid. For $0.81\lesssim x$ it marks a stable continuous $F-S_7$ phase transition. The circles are coexisting states taken from the simulation results in Ref. 40 and 41. Finally, the stars correspond to the states whose density profiles are represented in Figs. 13–16.

a fluid, while they should exhibit columnar ordering. Another interesting result is that, at approximately $\beta p\approx 0.24$, there appear a solid-solid phase separation between a small-particle-rich and a large-particle-rich phases. Finally, it is worth mentioning the existence of an extremely narrow chimney of S_6-C_6 coexistence. This suggests that the columnar phase is very sensitive to small perturbations.

As concerns the density profile in the ordered phases, we have chosen a few representative states of the system (marked with stars in Fig. 11) in order to illustrate the way large and small particles distribute in each phase. In Fig. 13 we show the density profiles for a period-7 solid phase for different sections perpendicular to the direction s_3. This size is one lattice spacing bigger than the size of the large particles. We can conclude from the figure that the large particles are arranged in such a way that the small ones can be accommodated between any two of them. So, we could say that the large particles in the unit cell are surrounded by the

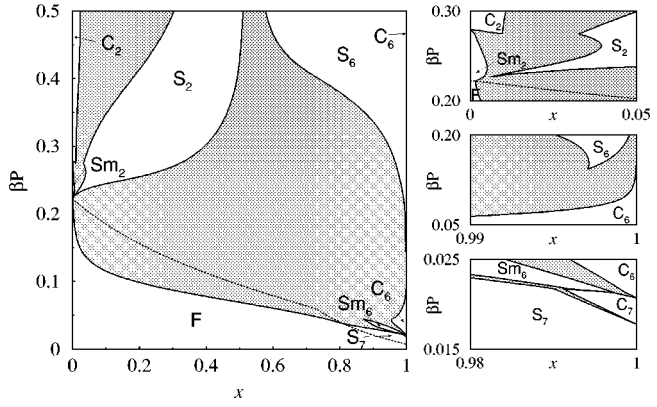

FIG. 12. Phase diagram (reduced pressure, βP, versus composition, x) of the same system refers in Fig. 11 (the labels used are the same as in that figure). Now coexisting tie lines are horizontal. The dotted line is the same as in the previous figure. Insets show some details of the phase diagram.

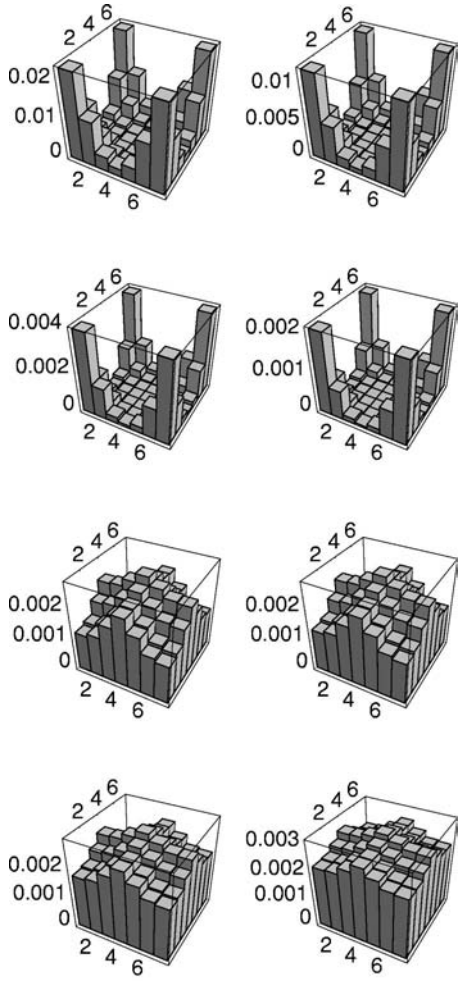

FIG. 13. Density profiles for a solid phase with periodicity $d=7$, corresponding to $\eta=0.56$, $x=0.97$ and $\beta p=0.02$. Different planar sections at $s_3=1,2,3,4$ (from top to bottom and from left to right) are plotted.

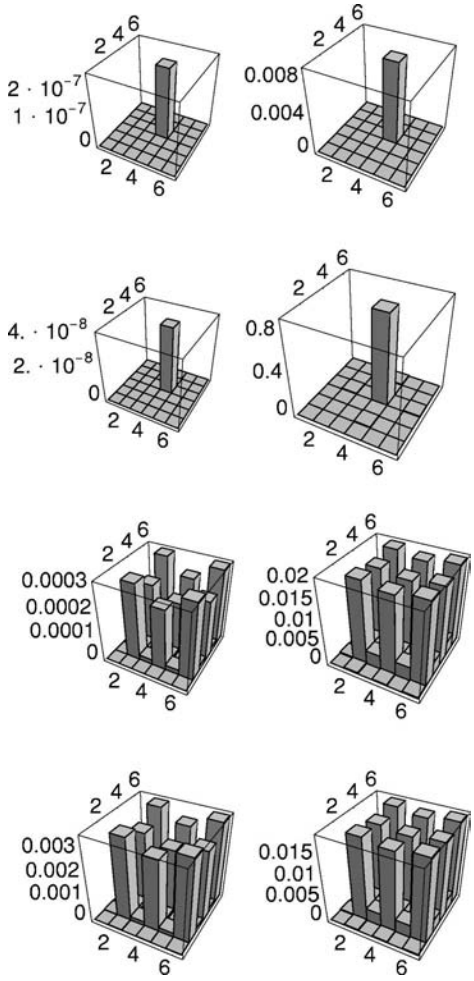

FIG. 14. Density profiles for a solid phase with periodicity $d=6$, corresponding to $\eta=0.989$, $x=0.973$ and $\beta p=0.265$. Different planar sections at $s_3=1,2,3,4$ (from top to bottom and from left to right) are plotted.

small ones. Note that the density of the latter does not change very much within the unit cell. In Fig. 14 the density profile for a period-6 solid is shown. It is very interesting to see that its structure is completely different to the previous one. Now, as the unit cell is of the same size of the large particles, the small ones can only be placed at vacant unit cells. Thus, the unit cell is completely filled with the small particles, which, as can be appreciated in the figure, form a crystal. Noticeably, the value of the small particle density is slightly higher at the contact with the large particles, which can be interpreted as an adsorption phenomenon. Figures 15 and 16 exhibit the profile of the period-6 column and smectic phases, respectively. From the discussion of the period-6 solid profiles we have just made, the interpretation of these two new density profiles should be straightforward.

IV. CONCLUSIONS

In this work we have applied the extension of FMT to lattice models[42] to study two systems already treated in the literature: the two-dimensional lattice gas with first and second neighbor exclusion on a square lattice, and the binary mixture of parallel hard cubes with edge-lengths $\sigma_L=6$ and $\sigma_S=2$ on a simple cubic lattice. For both systems we have shown a systematic way of using the theory in order to perform a complete calculation of the bulk phase diagrams. In particular, for the first system a very detailed analysis have been carried out. All the relevant thermodynamic functions can be analytically obtained within this approach, for both

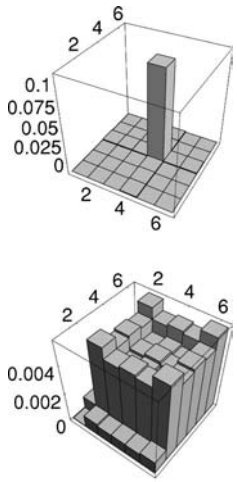

FIG. 15. Density profiles for a columnar phase with periodicity $d=6$, corresponding to $\eta=0.78$, $x=0.96$ and $\beta p=0.04$.

uniform and columnar phases. The results compare well with others previously obtained by different authors using widely accepted theoretical approaches. It is remarkable that, in spite of the simplicity of the treatment, the results obtained are rather accurate, specially in the low and high density limits.

On the other hand, a very complete study has been carried out for the three-dimensional system. The rich phase diagram obtained is very striking, considering the simplicity of both the system and the theory. There appear many different entropy-driven phase transitions: fluid-ordered phase demixing, one-, two- and three-dimensional ordering and solid-solid phase separation. The results obtained have also allowed to reinterpret the simulations results[40,41] in a way consistent with the general picture emerged during the last decade about demixing of additive hard-core binary mixtures: fluid-fluid demixing is always preempted by the ordering of one of the phases.

We have performed a free minimization of the functional and have thus obtained the structure of all the ordered phases. The results we get show that the density profile of the small particles is far from being uniform. In general, when dealing with three-dimensional models, a free minimization is not feasible, so the density profile must be properly parametrized. Since there is very little intuition about the density profiles of mixtures, the small components are always assumed to be uniformly distributed over the volume. According to our findings, this is definitely wrong. Perhaps our results can help to gain insight into what a proper parametrization of the density profiles looks like.

We would also like to emphasize that the LFMT is a mean-field-like theory, but not a trivial one. This can be understood if we realize that the direct correlation functions have finite range, which means that at some point the correlations between particles are neglected. This fact is reflected in the lower accuracy of the description around critical points. However, away from these regions the results are far more accurate than those obtained from a standard mean field theory, and what is even more important, at the expense of no much more work.

The study of lattice gases within the framework of density functional theory can be very fruitful, as we hope to have been able to transmit in this work. On the one hand, there is not loss in phenomenology or complexity of behaviors; on the other hand, the approach is considerably simpler numerically, something that allows one to tackle problems which have so far not been solved in continuum models. Besides, from a purely formal point of view, lattice density functionals reveal some structures which may be hidden in similar developments for continuum models. So, its careful analysis may reveal important properties of the latter in the near future. For these reasons we believe that it is very important to extend this kind of work to more general lattice models. We plan to report on that shortly.

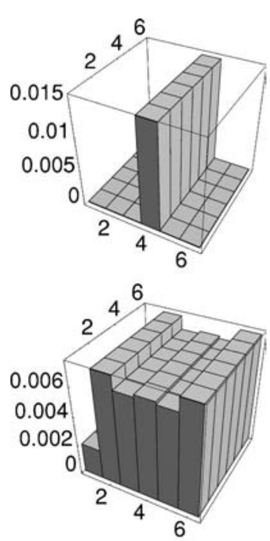

FIG. 16. Density profiles for a smectic phase with periodicity $d=6$, corresponding to $\eta=0.92$, $x=0.613$ and $\beta p=0.035$.

ACKNOWLEDGMENTS

This work is supported by Project No. BFM2000-0004 from the Dirección General de Investigación (DGI) of the Spanish Ministerio de Ciencia y Tecnología.

APPENDIX: DIAGRAMMATIC NOTATION: A THREE-DIMENSIONAL EXAMPLE

Let us consider a system of parallel hard cubes in a simple cubic lattice with edge-length $\sigma=2$. This system is equivalent to the lattice gas on a simple cubic lattice with first, second and third neighbor exclusion. The excess functional, in diagrammatic notation, can be written as

$\beta\mathcal{F}_{\rm ex}[\rho]=\sum_{\mathbf{s}\in\mathbb{Z}^3}[\Phi_0($ 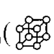 $)-\Phi_0($  $)-\Phi_0($ 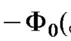 $)-\Phi_0($ 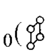 $)$
$+\Phi_0($  $)+\Phi_0($  $)+\Phi_0($  $)-\Phi_0($  $)],$ (A1)

where the diagrams represent the weighted densities

 $=n^{(1,1,1)}(\mathbf{s})=\sum_{i,j,k=0,1}\rho(s_1+i,s_2+j,s_3+k),$

 $=n^{(0,0,1)}(\mathbf{s})=\sum_{i=0,1}\rho(s_1,s_2,s_3+i),$

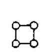 $=n^{(0,1,1)}(\mathbf{s})=\sum_{i,j=0,1}\rho(s_1,s_2+i,s_3+j),$

 $=n^{(0,1,0)}(\mathbf{s})=\sum_{i=0,1}\rho(s_1,s_2+i,s_3),$

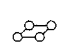 $=n^{(1,1,0)}(\mathbf{s})=\sum_{i,j=0,1}\rho(s_1+i,s_2+j,s_3),$

 $=n^{(1,0,0)}(\mathbf{s})=\sum_{i=0,1}\rho(s_1+i,s_2,s_3),$

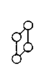 $=n^{(1,0,1)}(\mathbf{s})=\sum_{i,j=0,1}\rho(s_1+i,s_2,s_3+j),$

$$\circ = n^{(0,0,0)}(\mathbf{s}) = \rho(s_1, s_2, s_3).$$

In Ref. 42 it was pointed out that the family of approximate functionals constructed after the prescription of the lattice fundamental measure theory consistently satisfied the dimensional reduction property of the exact functionals. Hence, the functional (9) must be recovered from the functional (A1). To show it we can apply an infinite external potential in every site on the tridimensional lattice, except in the sites laying on the plane $\mathcal{P}=\{(0,s_2,s_3): s_2, s_3 \in \mathbb{Z}\}$. Then the different contributions to the effective excess functional become

$$\sum_{s_1 \in \mathbb{Z}} \Phi_0(\;) = 2\Phi_0(\;),$$

$$\sum_{s_1 \in \mathbb{Z}} \Phi_0(\;) = \Phi_0(\;),$$

$$\sum_{s_1 \in \mathbb{Z}} \Phi_0(\;) = 2\Phi_0(\;),$$

$$\sum_{s_1 \in \mathbb{Z}} \Phi_0(\;) = 2\Phi_0(\;),$$

$$\sum_{s_1 \in \mathbb{Z}} \Phi_0(\;) = \Phi_0(\;),$$

$$\sum_{s_1 \in \mathbb{Z}} \Phi_0(\;) = \Phi_0(\;),$$

$$\sum_{s_1 \in \mathbb{Z}} \Phi_0(\;) = 2\Phi_0(\;),$$

$$\sum_{s_1 \in \mathbb{Z}} \Phi_0(\;) = \Phi_0(\;),$$

and therefore Eq. (A1) reduces to Eq. (9).

This diagrammatic notation can also be extended to multicomponent systems, although for more than two components it becomes too cumbersome.

[1] L. Onsager, Ann. N.Y. Acad. Sci. **51**, 627 (1949).
[2] J. G. Kirkwood, E. K. Maun, and B. J. Alder, J. Chem. Phys. **18**, 1040 (1950).
[3] B. J. Alder and T. E. Wainwright, J. Chem. Phys. **27**, 1208 (1957).
[4] W. W. Wood and J. D. Jacobson, J. Chem. Phys. **27**, 1207 (1957).
[5] D. Frenkel, H. N. V. Lekkerkerker, and A. Stroobants, Nature (London) **332**, 822 (1988).
[6] J. A. C. Veerman and D. Frenkel, Phys. Rev. A **45**, 5632 (1992).
[7] P. Bolhuis and D. Frenkel, J. Chem. Phys. **106**, 666 (1997).
[8] B. Widom and J. S. Rowlinson, J. Chem. Phys. **52**, 1670 (1970).
[9] S. Asakura and F. Oosawa, J. Chem. Phys. **22**, 1255 (1954).
[10] B. Widom, J. Chem. Phys. **46**, 3324 (1967).
[11] D. Frenkel and A. Louis, Phys. Rev. Lett. **68**, 3363 (1992).
[12] J. L. Lebowitz and J. S. Rowlinson, J. Chem. Phys. **41**, 133 (1964).
[13] T. Biben and J.-P. Hansen, Phys. Rev. Lett. **66**, 2215 (1991).
[14] H. N. W. Lekkerkerker and A. Stroobants, Physica A **195**, 387 (1993).
[15] Y. Rosenfeld, Phys. Rev. Lett. **72**, 3831 (1994).
[16] W. C. K. Poon and P. B. Warren, Europhys. Lett. **28**, 513 (1994).
[17] C. Caccamo and G. Pellicane, Physica A **235**, 149 (1997).
[18] T. Coussaert and M. Baus, J. Chem. Phys. **109**, 6012 (1998).
[19] E. Velasco, G. Navascués, and L. Mederos, Phys. Rev. E **60**, 3158 (1999).
[20] A. Buhot and W. Krauth, Phys. Rev. Lett. **80**, 3787 (1998).
[21] M. Dijkstra, R. van Roij, and R. Evans, Phys. Rev. Lett. **81**, 2268 (1998).
[22] M. Dijkstra, R. van Roij, and R. Evans, Phys. Rev. Lett. **82**, 117 (1999).
[23] M. Dijkstra, R. van Roij, and R. Evans, Phys. Rev. E **59**, 5744 (1999).
[24] N. García-Almarza and E. Enciso, Phys. Rev. E **59**, 4426 (1999).
[25] P. D. Kaplan, J. L. Rouke, A. G. Yodh, and D. J. Pine, Phys. Rev. Lett. **72**, 582 (1994).
[26] A. D. Dinsmore, A. G. Yodh, and D. J. Pine, Phys. Rev. E **52**, 4045 (1995).
[27] U. Steiner, A. Meller, and J. Stavans, Phys. Rev. Lett. **74**, 4750 (1995).
[28] A. Imhof and J. K. G. Dhont, Phys. Rev. Lett. **75**, 1662 (1995).
[29] J. A. Cuesta, Phys. Rev. Lett. **76**, 3742 (1996).
[30] Y. Martínez-Ratón and J. A. Cuesta, Phys. Rev. E **58**, R4080 (1998).
[31] Y. Martínez-Ratón and J. A. Cuesta, J. Chem. Phys. **111**, 317 (1999).
[32] H. N. V. Temperley, Proc. Phys. Soc. **86**, 185 (1965).
[33] D. M. Burley, in *Phase Transitions and Critical Phenomena*, edited by C. Domb and M. S. Green (Academic, London, 1972), Vol. 2, Chap. 9, pp. 329–374.
[34] L. K. Runnels, in *Phase Transitions and Critical Phenomena*, edited by C. Domb and M. S. Green (Academic, London, 1972), Vol. 2, Chap. 8, pp. 305–328.
[35] R. Evans, in *Fundamentals of Inhomogeneous Fluids*, edited by D. Henderson (Dekker, New York, 1992), Chap. 3, p. 85.
[36] A. R. Denton and N. W. Ashcroft, Phys. Rev. A **42**, 7312 (1990).
[37] M. Dijkstra, Phys. Rev. E **58**, 7523 (1998).
[38] A. A. Louis, R. Finken, and J. P. Hansen, Phys. Rev. E **61**, R1028 (2000).
[39] P. Germain and S. Amokrane, Phys. Rev. E **65**, 031109 (2002).
[40] M. Dijkstra and D. Frenkel, Phys. Rev. Lett. **72**, 298 (1994).
[41] M. Dijkstra, D. Frenkel, and J.-P. Hansen, J. Chem. Phys. **101**, 3179 (1994).
[42] L. Lafuente and J. A. Cuesta, J. Phys.: Condens. Matter **14**, 12079 (2002).
[43] L. Lafuente and J. A. Cuesta, Phys. Rev. Lett. **89**, 145701 (2002).
[44] M. Nieswand, W. Dieterich, and A. Majhofer, Phys. Rev. E **47**, 718 (1993).
[45] M. Nieswand, A. Majhofer, and W. Dieterich, Phys. Rev. E **48**, 2521 (1993).
[46] D. Reinel, W. Dieterich, and A. Majhofer, Phys. Rev. E **50**, 4744 (1994).
[47] P. Tarazona and Y. Rosenfeld, Phys. Rev. E **55**, R4873 (1997).
[48] J. A. Cuesta and Y. Martínez-Ratón, Phys. Rev. Lett. **78**, 3681 (1997).
[49] F. H. Ree and D. A. Chesnut, Phys. Rev. Lett. **18**, 5 (1967).
[50] R. M. Nisbet and I. E. Farquhar, Physica (Amsterdam) **73**, 351 (1974).
[51] A. Bellemans and R. K. Nigam, J. Chem. Phys. **46**, 2922 (1967).
[52] A. Baram, J. Phys. A **16**, L19 (1983).
[53] A. Baram and M. Luban, Phys. Rev. A **36**, 760 (1987).
[54] P. A. Slotte, J. Phys. C **16**, 2935 (1983).
[55] B. Groh and B. Mulder, J. Chem. Phys. **114**, 3653 (2001).
[56] G. S. Rushbrooke and H. I. Scoins, Proc. R. Soc. London, Ser. A **230**, 74 (1955).
[57] J. A. Cuesta, Europhys. Lett. **46**, 197 (1999).